Engineering

Mechanical Engineering fields

Okayama University *Year* 2007

Sorption Characteristics of Honeycomb-Type Sorption Element Composed of Organic Sorbent

Hideo Inaba[*] Takahisa Kida[†]

Akihiko Horibe[‡] Makoto Kaneda[**]

[*]Okayama University

[†]Engineering Group, Engineering Division, Japan EXLAN Co., Ltd

[‡]Okayama University

[**]Engineering Group, Engineering Division, Japan EXLAN Co., Ltd

Sorption Characteristics of Honeycomb-Type Sorption Element Composed of Organic Sorbent*

Hideo INABA**, Takahisa KIDA***,
Akihiko HORIBE** and Makoto KANEDA***

This study deals with the sorption characteristics of a honeycomb-type sorption element composed of a new organic sorbent that was composed of the cross-linked polymer of sodium acrylate. Transient experiments in which moist air was passed into the honeycomb-type sorption element were conducted under various conditions of air velocity, temperature, relative humidity and honeycomb length. As a result, the effective mass transfer coefficient of the organic sorbent adsorbing the water vapor was non-dimensionalized as a function of Reynolds number, modified Stefan number and non-dimensional honeycomb length.

Key Words: Air Conditioning, Sorption, Organic Sorbent, Water Vapor, Honeycomb Shape, Mass Transfer

1. Introduction

In recent years, the rapid increase in the demand for energy has been brought about by the increase in energy consumption especially in terms of people day-to-day living and transportation. The majority of thermal energy used for domestic air conditioning and hot water supply lies in the low-temperature energy category below 100°C. On the other hand, the usage of fossil fuel for energy, which produces green house gas, has been increasing due to its low cost. One of the solutions to this problem is to effectively utilize the abundant low-temperature waste heat energy produced in manufacturing and peoples' daily living processes. This type of unused heat energy has been classified as a potential new energy source, which is cost free and environmentally friendly. Therefore, one of the candidate heat conversion machines, which is suitable for low-temperature heat sources and has a smaller load on the environment, is an adsorption refrigerator rather than a vapor compression refrigerator or heat pump using harmful refrigerants[1]. In general, inorganic adsorbents such as Silica-gel and Zeolite have been used for adsorption refrigerators[2]-[4]. However, this type of adsorption equipment has such some problems as the decrease in adsorption ability and the increase in flow resistance caused by the degradation phenomenon of powdering of inorganic adsorbents after the repetition use under the conditions of expansion and shrinkage of the adsorbent during the adsorption and desorption processes.

One suitable type of adsorbent for solving this problem in the case of the inorganic adsorbents is an organic adsorbent such as a sorption polymer. One of the candidate sorption polymers is a cross-linked polymer of sodium acrylate. This polymer containing the carboxyl group as a water vapor sorption site has a larger sorption capacity compared to Silica-gel. As a result of basic research concerned with the sorption and desorption characteristics of the cross-linked polymer of sodium acrylate which is processed like a fiber, the authors reported that there was a drawback in that the flow resistance increased[7].

In this study, for the purpose of developing the desiccant humidifier or desiccant cooling system[5]-[6], the effects of some parameters on sorption characteristics of the sodium acrylate adsorbent which were processed in a honeycomb shape were examined experimentally. The obtained results will enable us to develop the adsorption refrigeration machine.

* Received 12th October, 2001. Japanese original: Trans. Jpn. Soc. Mech. Eng., Vol. 66, o. 652, B (2000), pp. 3204-3211 (Received 12th December, 1999)

** Okayama University, Graduate School of Natural Science and Technology, 3-1-1 Tsushimanaka, Okayama-City 700-8530, Japan. E-mail: inaba@mech.okayama-u.ac.jp

*** Engineering Group, Engineering Division, Japan EXLAN Co., Ltd., 3-3-1 Kanaoka-Higashimachi, Okayama-City 704-8510, Japan

Nomenclature

A: area [m²]
C_p: specific heat of air at constant pressure [kJ/(kg•K)]
D: diffusion coefficient [m²/s], diameter of the pipe [mm]
d: particle diameter of the sorbent [mm]
d_e: hydraulic diameter of honeycomb pass [mm]
H: enthalpy unit time [kJ/s]
h: specific enthalpy [kJ/kg]
h_m^*: effective mass transfer coefficient [m/s]
i: time step
L: honeycomb length [m]
L_s: sorption heat [kJ/kg]
M: mass flow rate [kg/s]
m: mass [kg]
Po: atmospheric pressure [Pa]
p: pressure [Pa]
R: gas constant [kJ/(kg•K)]
r: radius of fine pore [nm]
S: surface area [m²]
T: absolute temperature [K]
t: time [s]
u: air velocity [m/s]
V: volume [m³]
x: absolute humidity [kg/kg']
ρ: density [kg/m³]
θ: temperature [°C]
Δt: time interval [s]
ϕ: relative humidity [%]
ν: kinetic viscosity [m²/s]

subscripts:

a: dry air
as: between air and water vapor
in: inlet of the test section
ini: initial condition
$loss$: loss
m: mean
o: dry condition or flowing condition
out: outlet of the test section
s: saturated water vapor
w: water vapor
$*$: modified value

2. Features of the Present Polymer Sorbent

2.1 Features of the cross-linked polymer of sodium acrylate

Figures 1(a) and 1(b) show the chemical structure and microphotograph (×1 000 magnifications) of the present polymer of sodium acrylate with a cross-linking structure consisting of tetrazine, which has four nitrogen atoms. Water vapor molecules are adsorbed into the sodium acrylate sites on a side-chain of the polymer with increasing volume. Thus, this phenomenon, in which the sodium acrylate site adsorbs water vapor molecules by a weak force with deformation of its shape, is called "Sorption"[3], and it is able to desorp the water vapor from the adsorption sites under the low-temperature condition. The sorption heat (L_s=2 500 kJ/kg) is almost the same as the condensation heat of water vapor. The temperature level for desorping water vapor from the sorption site ranges from 45 to 80°C.

In the present study, for the purpose of applying the present organic sorbent to the rotary-type desiccant humidifier or desiccant cooling system, the organic sorbent powder was coated to a pulp sheet of 0.26 mm thickness and then the pulp sheet was processed into a honeycomb cell having a triangular cross section of cylindrical shaped honeycombs of diameter D=38 mm, as shown in Fig. 2. The hydraulic diameter of the honeycomb cell is determined as d_e=1.77 mm in consideration of the optimum sorption area and air flow resistance. Mean diameter of the sorbent particles is d=60 μm. From the result of the endur-

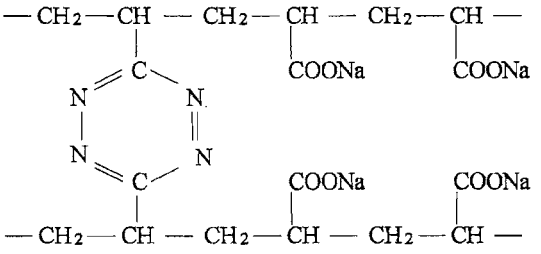

Fig. 1(a) Chemical structure of test sorbent particle

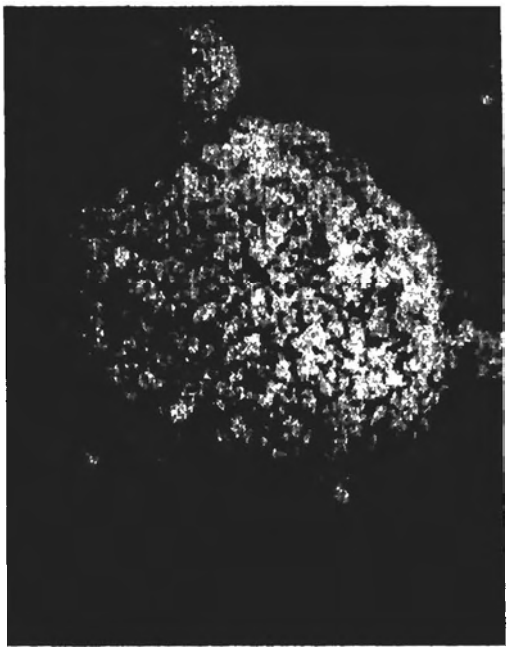

Fig. 1(b) Microphotograph of test sorbent particle

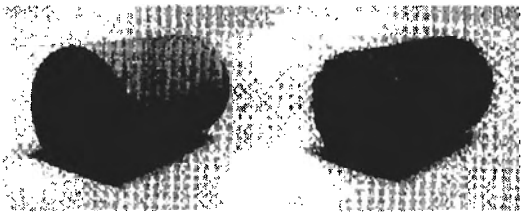

Fig. 2 Appearance of honeycomb sorbent sample

ance test of the honeycomb element by repeated sorption and desorption processes, the dropout of sorbent particles from the pulp sheet was not observed.

Three kinds of cylindrical honeycombs of different length L=60, 120 and 200 mm were selected in the present study.

2.2 Pore size distribution of the sorbent particles

The sorption characteristic of the water vapor from the moist air is influenced by the external diffusion based on the concentration boundary layer growing near the surface of the sorbent particles and the internal diffusion based on the pore of the sorbent particles. In particular, the pore morphology of the sorbent particle exerts a significant influence on the internal diffusion in relation to the sorption characteristics. The pore size distribution of the sorbent particles was measured by the mercury press-injection method and nitrogen permutation method. The measured pore size was distributed from 4×10^{-3} nm to 60 nm, which was ranged from the molecular diffusion area to Knudsen diffusion area. On the other hand, the pore size of the commercial Silica-gel ranged from 10 nm to 8×104 nm, which belonged to the molecular diffusion area.

2.3 Static sorption equilibrium characteristics

The static sorption equilibrium was measured using the saturated salt method[7]. The data of net sorption weight m_w under the various relative humidity conditions were obtained. Moreover, the static sorption equilibrium of Silica-gel as an inorganic sorbent (hydraulic diameter d_e=1.56 mm) was also measured. The non-dimensional quantities, m_w/m_0, (m_0: honeycomb weight under the complete dry condition) against the relative humidity ϕ(%) are plotted in Fig. 3. It is noted that the m_w/m_0 of the present organic sorbent is more than twice that of the Silica-gel. The m_w/m_0 of the present organic sorbent increases almost linearly with increasing relative humidity ϕ.

3. Experimental Apparatus and Procedure

3.1 Experimental apparatus

The schematic of the present experimental apparatus is shown in Fig. 4. The present apparatus was composed of an air compressor, after cooler, filtering

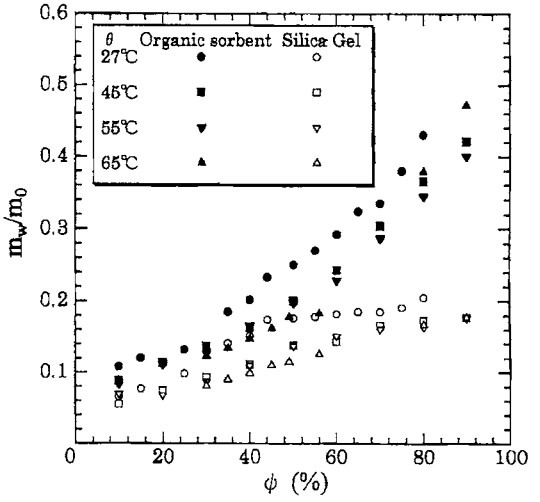

Fig. 3 Sorption isotherm

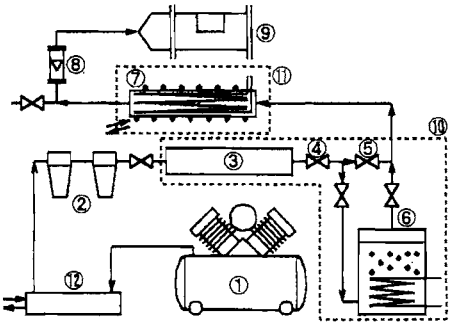

Fig. 4 System diagram of apparatus

section, humidity control section, temperature control section, pendulum flow meter, and cylinder type test section in which the sorbent honeycomb was installed. Compressed air which was discharged from the oil-less air compressor (maximum power output: 3.7 kW, maximum discharge pressure: 0.83 MPa, maximum discharge volume: 67 m³/sec) flowed into the filtering section after being cooled by a water-cooled cooling unit. This filtering section consisted of an air filter which could remove impurities below 0.3 μm in diameter and a micromist filter which could remove impurities below 0.01 μm in diameter. The compressed air, after passing through two filters, arrived at the humidity control section that was composed of a membrane-type dehumidifier and a bubble-tower-type humidifier. At the bubble-tower-type humidifier, the air was injected into the hot water layer from the dispersion plate having fine holes at the bottom of the test cylinder. The air bubbles generated in the hot

water layer and the ascending air bubbles were humidified. The humidity of the air was adjusted by using the membrane-type dehumidifier and the bubble-tower-type humidifier. The temperature control section is composed of an electric heater (maximum output: 1.5 kW) installed in the stainless pipe which was covered with a thermal insulator (glass wool of 50 mm thickness) and a copper tube wrapped around the stainless pipe in order to supply brine. The electric power supplied to an electric heater was adjusted by the PID control method based on the electric output of a K-type thermocouple set at the entrance. The air controlled at constant temperature and humidity arrived at the bottom of the test section through the pendulum flowmeter (flow rate range: $5\times10^{-4}\sim5\times10^{-3}$ m^3/sec).

The details of the test section are shown in Fig. 5. The main part of the test section was a cylindrical vessel that was made from vinyl chloride and was covered with glass wool insulator of 50 mm thickness. A hatch cover was installed at the center of the test cylinder in order to insert or remove the honeycomb. The sponge was stuck to the inner wall of the cylindrical test vessel for thermal insulation. As shown in Fig. 5, some holes for measuring static pressure, thermocouples for measuring temperature and a humidity detector (hygrometer) were equipped near the inlet and outlet of the test section. The holes for measuring static pressure were connected to the manometer and the pressure difference detector of air flow. Temperatures of the inlet and outlet of the test section were measured by K-type thermocouples whose wire diameter was 0.3 mm, and measuring accuracy was ±0.1 K. A thin film polymer-type static electricity capacitance detector (measuring accuracy of $\pm2\%$) for measuring the air humidity and a mirror surface cooling-type dew point monitor (measuring accuracy of ±0.2 K) were used in the present measurement. Three kinds of cylindrical honeycomb samples having different lengths of L=60 mm, 120 mm and 200 mm were used to examine the length effect of the test honeycomb.

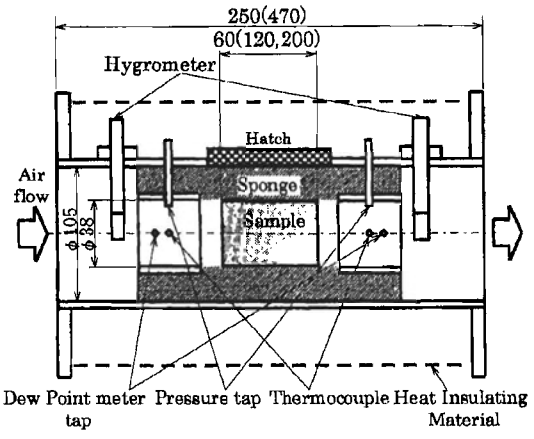

Fig. 5 *Detail of test section*

The inflow enthalpy time variation ($H_{in}=M\times h_{in}$) and the outflow enthalpy time variation ($H_{out}=M\times h_{out}$) of the moist air to the honeycomb sorbent were calculated from the mass flow rate of the air M and specific enthalpy h which were derived from the measured values of the air temperature and humidity, specific heat, and latent heat of water vapor. The enthalpy variation of the honeycomb sorbent for each time interval h_f was estimated from the measured values from six thermocouples installed in the test section. The enthalpy time variation of the adsorbed water ΔH_w was calculated from the specific heat of water and mean temperature of the sorbent after measuring the amount of adsorbed water weight at each time interval. Moreover, the heat loss Q_{loss} from the test section for each time interval was estimated from the data of the heat flux detector installed at the outside wall surface of the cylindrical test section. From the results of a preliminary experiment, it was clarified that the heat and the mass preservation in each test run was satisfied since the enthalpy difference between inflow and outflow air was consistent with total enthalpy variation of other elements.

3.2 Experimental method

The experiments were performed according to the following experimental procedures. First, the compressor was started, after that, the flow rate of air was set to a desired value and the air was passed through the test section after the air temperature and humidity were controlled at a constant value. Then, the hatch installed in the central part of the test section was opened, and the honeycomb sorbent was quickly set in the test section. The temperature and humidity of the test section and the temperatures of other elements were recorded by the data acquisition system at 10 sec intervals. The adsorbed water weight of the honeycomb sorbent was measured with an electronic scale by measuring the total weight of the honeycomb sorbent after taking it out from the hatch at a constant time interval. The honeycomb was rapidly returned to the test section within 5 sec and the experiment was continued.

4. Experimental Results and Consideration

4.1 Pressure loss characteristics of the honeycomb sorbent

The relation of air flow pressure loss ΔP [Pa] through the test honeycomb length L=60 mm and mean air flow velocity u_0 [m/s] in the honeycomb cell of hydraulic diameter d_e=1.77 mm is presented in Fig.

6. The pressure losses ΔP of the moist air flow were measured under the inflow air condition at the inlet temperature of θ_{in}=27°C and the air relative humidity of ψ_{in}=44% and 80%. The solid line in Fig. 6 was derived from the common pressure loss equation[9] of Hargen-Poiseuille's laminar flow for a smooth pipe (inner diameter of d=1.77 mm). The sorbent particles having average diameter d=60 μm were applied on the surface of the honeycomb cell. It is seen that the pressure loss of the air flow at relative humidity ψ_{in}=44% is 10~20% greater than that of a smooth-surface pipe since the air flow resistance increases with an increase in the surface roughness due to the sorbent particles on the honeycomb cell surface. As the relative humidity of the moist air increases from ψ_{in}=44% to 80%, the pressure loss ΔP from ψ_{in}=44% (open circle) to 80% (close circle) increases with an increase in the number of irregularities of honeycomb cell surface due to the swelling of the adsorbent particles.

4. 2 Sorption characteristic of the honeycomb cell sorbent exposed to a moist air flow

4. 2. 1 Unsteady-state sorption characteristic of the honeycomb cell sorbent The test standard conditions of inflow air temperature and humidity by JIS (Japanese Industrial Standard) were adopted in the present experiment. Inflow air flow velocities were selected according to the air flow condition of the commercial desiccant cooling unit, that is inflow air temperature of θ_{in}=27°C, inflow air relative humidity of ψ_{in}=44% and air flow velocity of u_0=2.0 m/s.

The time histories of various parameters such as inlet and outlet air temperature (θ_{in} and θ_{out}) and air humidity (ψ_{in} and ψ_{out}), net mass of sorbed water vapor m_w, non-dimensional amount of sorbed water vapor m_w/m_0, the ratio of the sorbed water vapor to the volume of the honeycomb cell m_w/V_0 under the initial condition of honeycomb cell temperature of θ_{ini}=65°C, honeycomb cell humidity of ψ_{ini}=8.4% are shown in Fig. 7(a). Figure 7(b) shows time histories of various parameters like those in Fig. 7(a) for a Silica-gel honeycomb cell.

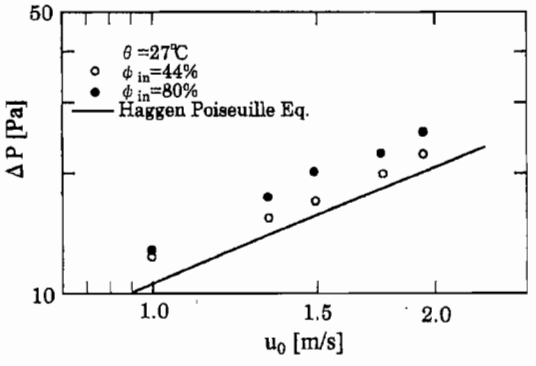

Fig. 6 Pressure loss of honeycomb cell

First, with respect to the air humidity variations, the outlet air humidity ψ_{out} decreases rapidly after the experiment starts against the inlet air humidity ψ_{in}. It is seen that the sorption processs of water vapor progressed rapidly at the beginning of the test run. After the value of ψ_{out} reaches a minimum, it increases gradually with time. Finally the value of ψ_{out} approaches that of the inlet air relative humidity ψ_{in}. On the other hand, values of m_w, m_w/m_0 and m_w/V_0 increase markedly after the experiment begin, and the rates of increase of those parameters decrease with time, and eventually reach the sorption equilibrium conditions. The sorption of water vapor into the sorbent progresses rapidly at the beginning of the test run since the water vapor concentration difference between the sorbent and moist air reaches the maximum value. As time progresses, the water vapor concentration difference between the sorbent and moist air is reduced. That is, the driving power of the sorbent decreases with time and the sorption processes approach the sorption equilibrium condition.

Secondary, concerning the outlet air temperature variation, the outlet air temperature θ_{out} increases rapidly at the beginning of the test run. After that, the value of θ_{out} decreases with time and finally approaches the inlet air temperature θ_{in}. This temperature behavior means that the amount of sorption increases in the first stage of the experiment and the outlet air temperature θ_{out} increases since a lot of sorption heat is generated in the sorption process. As time progresses the value of θ_{out} decreases with the heat generated due to the decrease in the amount of sorbed water vapor. Finally the heat generation ceases in the state of sorption equilibrium and the value of θ_{out} equals θ_{in}.

The time period for reaching 95% of the whole sorbed water vapor mass under the sorption equilibrium condition was defined as sorption completion time t_f and the results are plotted in Figs. 7(a), 7(b). The sorption completion times of t_f=11.2 min (the present sorbent) and t_f=11.0 min (Silica-gel) are also shown in these figures. On comparison of each parameter such as m_w, m_w/m_0 and m_w/V_0 between the present sorbent and Silica-gel, it is noticed that the obtained values of the present sorbent are 2.1 times, 1.6 times, 1.9 times greater, respectively, than those of Silica-gel.

The time histories of the accumulated enthalpy and heat such as inflow enthalpy change in the inlet air $\Sigma H_{in}\,\Delta t$, the accumulated outflow enthalpy change in the outlet air $\Sigma H_{out}\,\Delta t$, the enthalpy change in the honeycomb cell ΔH_f, the enthalpy change in adsorbing

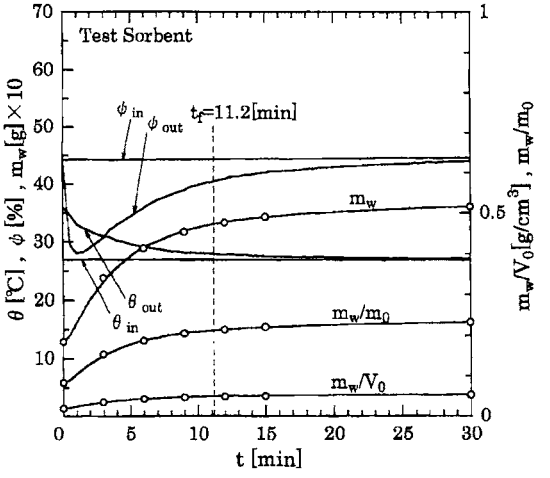

Fig. 7(a) Time history of each parameter for organic sorbent

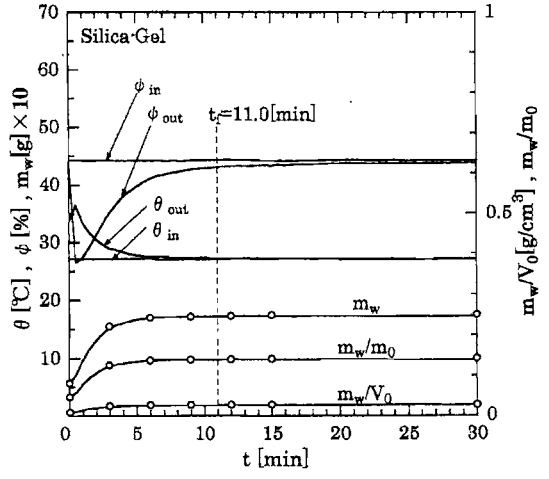

Fig. 7(b) Time history of each parameter for Silica-gel

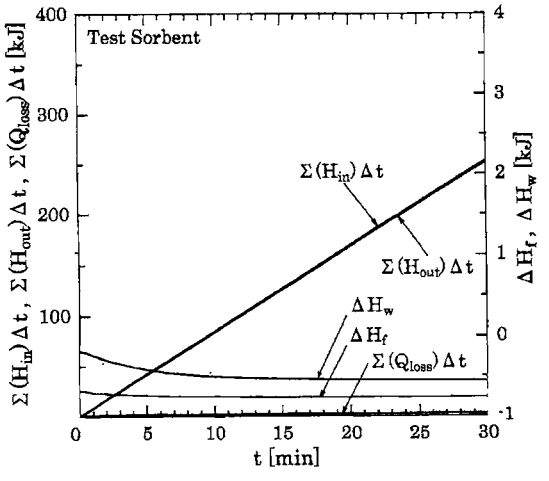

Fig. 7(c) Time history of heat for organic sorbent

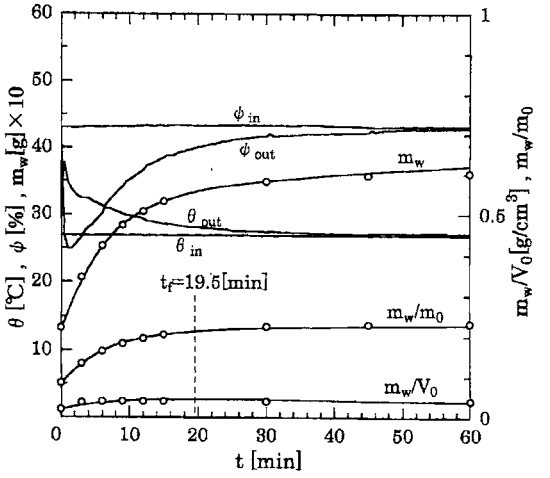

Fig. 8 Time history of each parameter for u_0=1.0 m/s

water vapor ΔH_w, and the accumulated heat loss from the test section to the environment $\Sigma Q_{loss}\,\Delta t$ are plotted in Fig. 7(c).

It is understood from Fig. 7(c) that the accumulated inflow enthalpy in the inlet air $\Sigma H_{in}\,\Delta t$ is almost equal to the accumulated outflow enthalpy in the outlet air $\Sigma H_{out}\,\Delta t$. It is seen that the enthalpy change in honeycomb cell ΔH_f in the first stage of the experiment is negligible, after which it reaches almost a constant value in the latter half of the experiment since the temperature decreases gradually from the initial condition of θ_{ini}=65°C due to the greater heat capacity of the honeycomb cell. The interaction of temperature decrease of the sorbent from the initial condition and increases in the amount of adsorbing water vapor and adsorption heat influence the enthalpy change in adsorbing water vapor ΔH_w in the initial stage of the experiment.

4.2.2 Effect of inflow air velocity Figure 8 shows the sorption characteristics of the present honeycomb cell in the case of the inflow air velocity u_0= 1.0 m/s instead of u_0=2.0 m/s as the basic condition. As the inflow air velocity decreases from u_0=2.0 m/s to u_0=1.0 m/s, the concentration boundary layer around the honeycomb cell surface is reduced. Therefore, the amount of sorbed water vapor decreases due to the decrease in external mass diffusion coefficient by forced convection. It is noted from in Fig. 8 that the sorption phenomenon progresses gradually and the sorption completion time t_f is 1.7 times as that at u_0=2.0 m/s. The decrease in air flow velocity allows a reduction in the diffusion effect of the sorption heat generated. As a result, the maximum air temperature at the exit of the test honeycomb cell θ_{out} increases from 37.5°C at u_0=1.0 m/s to 35.2°C at u_0=1.0 m/s. The time period to reach the maximum temperature

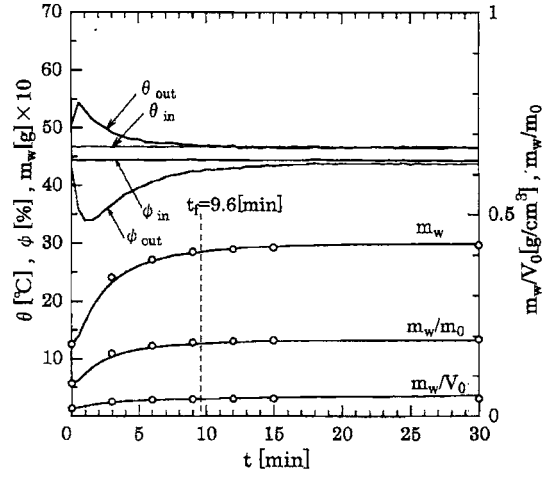

Fig. 9 Time history of each parameter for θ_{in}=47°C

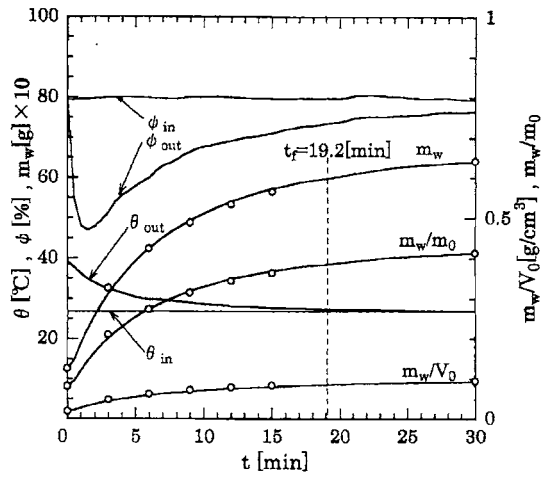

Fig. 10 Time history of each parameter for ϕ_{in}=80%

of air increases with a decrease in inflow air velocity.

4. 2. 3 Effect of inflow air temperature Figure 9 presents various sorption data with time in which the inflow air temperature θ_{in} is varied from 27°C to 45°C. As indicated in Fig. 3, the amount of water vapor sorption m_w decreases with increasing the equilibrium air temperature. The non-dimensional amount of sorbed water vapor m_w/m_0 under various equilibrium conditions could be obtained by extrapolating from the sorption relation shown in Fig. 3. It is seen from Fig. 9 that the value of m_w/m_0 at θ_{in}= 47°C is 0.18 and it indicates a 22% decrease in the amount of sorbed water vapor as compared with the value of m_w/m_0=0.23 at θ_{in}=27°C. The sorption completion time is shortened at t_f=9.6 sec and it is 14% shorter than that of t_f=11.2 sec under the basic condition.

4. 2. 4 Effect of inflow air humidity Figure 10 shows various sorption data with time in which the inflow air humidity ϕ_{in} is varied from 44% to 80%. Under this high humidity condition, Δm_{wf} (the increment of the amount of sorbed water vapor from the start of the test run until sorption completion time t_f) becomes 4.73 g for ϕ_{in}=80% and the value of Δm_{wf} is 2.38 times greater than that of Δm_{wf}=1.98 g for ϕ_{in}= 44%. However the sorption completion time t_f becomes 19.2 sec and it is approximately 1.7 times longer than that of t_f=11.2 sec for ϕ_{in}=44%. The maximum outlet air temperature θ_{out} reaches 38°C just after the experiment starts and this corresponds to a temperature increment of about 3°C as compared with that of θ_{out}=35.2°C for ϕ_{in}=44% of the basic condition.

4. 2. 5 Effect of honeycomb length Figure 11 shows various sorption data with time in which the honeycomb length L is varied from L=60 mm to 200 mm. The value of Δm_{wf} for L=200 mm becomes 7.80

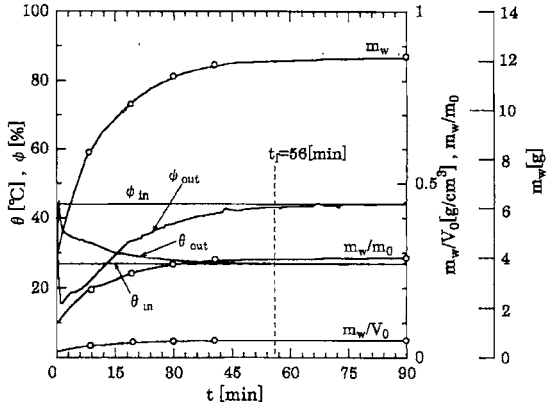

Fig. 11 Time history of each parameter for L=200 mm

g and Δm_{wf} is increases significantly compared to that for L=60 mm. In addition, the sorption completion time t_f for L=200 mm becomes 56 sec, whereas, the value of t_f is 11.2 sec for L=60 mm. As the honeycomb length increases, the sorption completion time for L=200 mm increases about five fold compared to that for L=60 mm since the water vapor concentration boundary layer develops thickly on the surface of the honeycomb cell in the downstream direction. The outlet air temperature θ_{out} reaches 44.5°C since total sorption heat increases with an increase in sorption area for L=200 mm.

4. 3 Mass transfer characteristics of the present honeycomb cell sorbent

In this chapter, the mass transfer coefficient of the sorbent is expressed from the experiment data and the non-dimensional correction equation is derived. Effective mass transfer coefficient h_m* shown in Eq. (1) was defined in consideration of total treatment of obtained data proposed by the Ref.(4).

$$h_m^*=\frac{1}{i}\sum_{n=1}^{i}\left\{\frac{1}{s(\rho_{in}-\rho_{wo}^*)}\left(\frac{\Delta m_w}{\Delta t}\right)i\right\} \quad (1)$$

where, i: the number of time interval, s: total surface area of the honeycomb cell (s=0.163 m^2), ρ_{in}: water vapor density of inflow air, ρ_{wo}: water vapor density of air surrounding honeycomb cell under the initial condition, and Δm_w: the amount of sorped water vapor during time interval Δt. Sherwood number Sh as a non-dimensional number of effective mass transfer coefficient h_w^* which is obtained from Eq. (1) was defined as follows.

$$Sh=\frac{h_m^* d_e}{D_{as}} \quad (2)$$

where, d_e: hydraulic diameter of honeycomb cell, and D_{as}: molecular diffusion coefficient of the air and water vapor[10].

The non-dimensional parameters that exert an influence on the Sherwood number were derived by using the dimension analysis method and considering the various above-mentioned factors. Reynolds number Re that represents the air flow behavior was adopted as a non-dimensional number in the air flow condition related to the external diffusion coefficient of the sorbent.

$$Re=\frac{u_0 d_e}{\nu} \quad (3)$$

Referring to the enthalpy of moist air composed of sensible heat and latent heat of the inflow air relates also to the expansion and the shrinkage of the sorbent which exert an influence on the mass transfer coefficient. The modified Stefan number Ste^* which is included with the sorption heat of water vapor Ls (= 2 500 kJ/kg) was defined as the ratio of sensible and latent heat of inflow air to the sorption heat generated in the sorption processs.

$$Ste^*=\frac{H_{in}}{M\cdot L_s}=\frac{c_{pa}\theta_{in}+x(L_s+c_{pw}\theta_{in})}{L_s} \quad (4)$$

Moreover, the ratio L/d_e of honeycomb length L to the hydraulic diameter of honeycomb cell d_e was adopted as a non-dimensional number of honeycomb cell dimension. The L/d_e relates to the external diffusion coefficient based on the boundary around the honeycomb cell. Schmidt number Sc as the physical properties of the moist air was assumed to be proportional to the 1/3th power of Sherwood number Sh, referring to the previous results[10].

The relationship between Sherwood number Sh and Reynolds number Re is shown in Fig. 12. The Sherwood number Sh increases with an increase in Re number. It is understood that the decrease in boundary layer thickness according to the increase in air flow velocity and the increase in the amount of inflow water vapor provide the increase of external diffusion coefficient related to the effective mass transfer

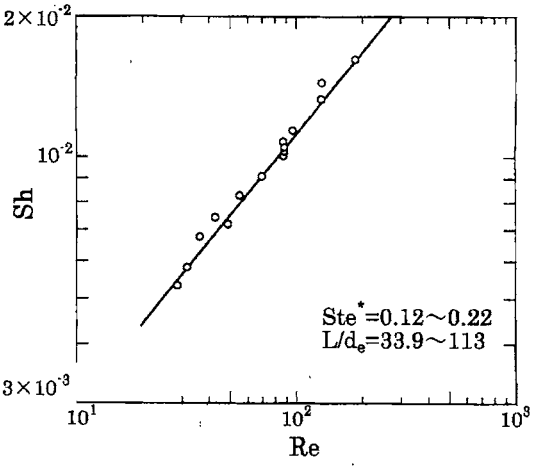

Fig. 12 Relationship between Sh and Re

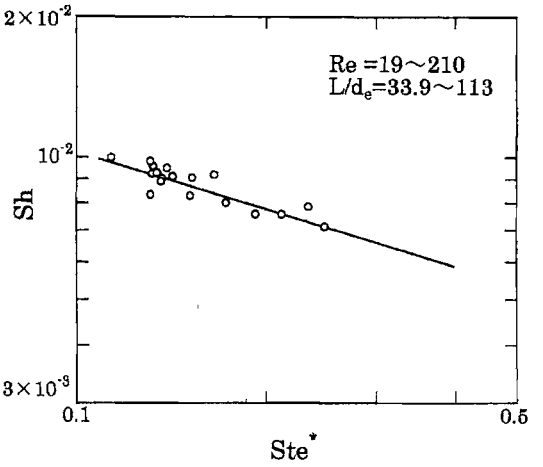

Fig. 13 Relationship between Sh and Ste^*

coefficient. In Fig. 12, the gradient of Sh to Re is about 0.68 and it is greater than that of 0.5 in common mass transfer of smooth surfaces without the sorption phenomenon, since the surface roughness of the honeycomb cell surface by sorbent particles provides the increase in turbulence intensity of air flow.

The relationship between Sherwood number Sh and modified Stefan number Ste^* is shown in Fig. 13. It is seen that Sherwood number Sh decreases with increasing modified Stefan number Ste^* as a non-dimensional amount of the enthalpy of inflow air. This tendency can be explained as follows. The increase in the inflow air enthalpy H_{in} during a time interval is caused by the increase of sensible heat which depends on the air temperature and the increase of latent heat which depends on humidity in the air as shown in Eq. (4). Initially, under air flow at a lower temperature, the temperature of the honeycomb cell under the initial temperature condition of θ_{ini}=65°C decreases with the progress of the sorption process

and the sorption ability increases gradually as shown in Fig. 3. While under air flow at a higher temperature, the amount of the water vapor sorption of the honeycomb cell decreases due to the decrease in temperature difference between the initial honeycomb cell temperature and inflow air temperature. From the viewpoint of an increase in the air temperature regarding the sorbent structure in detail, the sorbent particle volume expands gradually with increasing air temperature. That is, it is seen that the enhancement of the apparent mass transfer coefficient is caused by an increase in the irregularity of the honeycomb cell surface due to the expansion of the sorbent particles. Concerning the effect of air humidity, the increase in air humidity allows the amount of sorbed water vapor to increase as shown in Fig. 3. The expansion of the sorbent particles with an increase in the amount of sorbed water vapor was observed by the variation in pressure loss in Fig. 6, and this expansion of the sorbent particles causes the irregularity of honeycomb cell surface and the increase in the amount of the sorbed water vapor. As a result, the increase in the enthalpy, that is, the increase in modified Stefan number Ste^* allows to decrease the amount of sorbed water vapor, that is, to reduce Sherwood number Sh.

The relationship between Sherwood number Sh and non-dimensional number of honeycomb cell dimension L/d_e is shown in Fig. 14. It is noted from Fig. 14 that the thickness of the water vapor concentration boundary layer increases gradually with an increase in L/d_e, and Sherwood number Sh decreases since the ratio of sorption surface region having a low mass transfer coefficient, which occupies the whole honeycomb cell decreases with increasing length L. From Fig. 14, it is understood that the gradient of Sh to L/d_e is equal to -0.65. From the above-mentioned results, non-dimensional correlation equation of Sherwood number Sh was derived within an average deviation of $\pm 5\%$ by the least squares method as follows.

$$Sh=3.14\times10^{-3}\,Ste^{*-0.44}Re^{0.68}\left(\frac{L}{d_e}\right)^{-0.58}Sc^{1/3} \quad (5)$$

Applicable ranges in Eq. (5): $Ste^*=0.12\sim0.22$, $Re=19\sim210$, $L/de=33.9\sim113$, $Sc=0.510\sim0.581$

5. Concluding Remarks

By using the cross-linked polymer of sodium acrylate as a new type of polymer sorbent, effects of factors on the sorption characteristics were clarified as follows.

(1) From the measurement results of the sorption isotherm equilibrium of a new type of polymer sorbent of the cross-linked polymer of sodium acrylate, the amount of sorbed water vapor of the polymer sorbent is approximately 1.3 to 2.4 times greater than the inorganic adsorbent of Silica-gel.

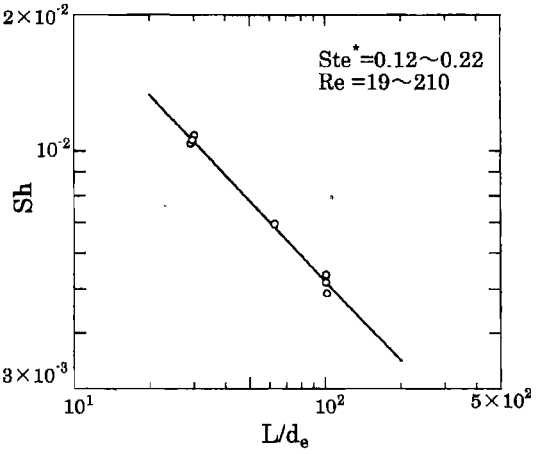

Fig. 14 Relationship between Sh and L/d_e

(2) For using the present polymer sorbent at an open-cycle such as humidity control or desiccant cooling system, the air flow resistance when the moist air is passed through the honeycomb cell sorbent was measured. It was seen that air flow resistance increased with increasing flowing air humidity due to the expansion of the sorbent particles.

(3) The effects of inflow air velocity, temperature, humidity, and honeycomb cell dimension on the unsteady-state sorption characteristic were clarified quantitatively. Moreover the non-dimensional correlation equation of the effective mass transfer coefficient was derived in terms of various parameters.

References

(1) Inaba, H., Energy New Technology Outline (edited by Kurosaki. Y.), Adsorption Type Refrigerator, (1998), pp. 781-791, N.T.S Pub. Co.
(2) Suzuki, M., Adsorption Engineering, (1990), pp. 26-35, Kodansha Pub. Co.
(3) Kondou, S., Chemistry Seminar 16, Chemistry of Adsorption, (1990), pp. 90-92, Maruzen Pub. Co.
(4) Yanai, H., Adsorption Engineering, (1977), pp. 59-65, Kyoritsu Pub. Co.
(5) Fedorov, A. and Viskanta, R., Heat Transfer Research, Vol. 36, No. 140 (1997), pp. 4-15.
(6) Watanabe, M., 25th Symposium on Heat Transfer 1988 in Japan, pp. 154-155.
(7) Inaba, H., Thermal Science and Engineering, Vol. 6, No. 1 (1999), pp. 11-18.
(8) Japanese Industrial Standard (JIS), C 9612, Room Air Conditioner, (1994), pp. 14-15.
(9) Thermal Design Method for Heat Exchanger, (1996), pp. 35-38, JSME.
(10) Seki, N., Heat Transfer Engineering, (1988), pp. 186-187, Morikita Pub. Co.